Available online at www.sciencedirect.com
SCIENCE DIRECT®
Journal of the European Ceramic Society 25 (2005) 335–348
www.elsevier.com/locate/jeurceramsoc

A comparison study of tialite ceramics doped with various oxide materials and tialite–mullite composites: microstructural, thermal and mechanical properties

Athena Tsetsekou*

Department of Mineral Resources Engineering, Technical University of Crete, 73100 Chania, Greece

Received 18 October 2003; received in revised form 6 March 2004; accepted 13 March 2004
Available online 21 July 2004

Abstract

Tialite (Al_2TiO_5) is a material of very low thermal expansion coefficient, high thermal shock resistance, high refractoriness and good corrosion resistance. However, its applications are very limited due to its low mechanical strength and to its thermal instability in the temperature range 750–1350 °C, which leads to the decomposition of the material to its parent oxides alumina and rutile. To overcome both problems, stabilization of the structure is tried through doping with various oxides; in the present work, a comparison study of the properties that can be achieved and of the decomposition behavior of tialite ceramics stabilized by adding MgO, talc or feldspar and of tialite–mullite composites made by the addition of kaolin is carried out. The processing conditions are also investigated for preparing porous ceramics for applications in the area of soot traps and hot gas clean-up. It was found that talc addition has an excellent stabilizing behavior, whereas tialite–mullite composites exhibit increased strength. Such composites with 10–20 wt.% mullite present the appropriate properties for the applications under consideration. Mullite presence also brings a stabilizing effect, thus in combination with talc additions it could lead to a very stable product.

Keywords: Tialite; Al_2TiO_5; Composites; Stabilization; Talc; Thermal expansion coefficient; Strength; Porosity; Microstructure

1. Introduction

Aluminum titanate (tialite) is a refractory material with very low thermal expansion coefficient (lower than that of fused silica), exhibiting as a consequence excellent thermal shock resistance. Additionally this material has very low thermal conductivity (of the order of $1.5\,W\,m^{-1}\,K^{-1}$) and high melting point (about 1860 °C).[1–3] These properties make it an excellent candidate material for refractory applications in the non-ferrous metallurgical industries, in the automotive industries for applications as exhaust port liners in automotive engines or as insulating components to increase heat efficiency[4] such as exhaust manifold inserts, piston crowns and turbocharger liners where both thermal insulation and thermal shock resistance are required[1,5,6] or even as thermal barriers.[7] Furthermore, its high thermal shock resistance, high refractoriness and good corrosion resistance are potentially advantageous for soot traps for diesel engines and filters for hot gas clean-up applications.[8–10]

However, these potential applications of this material have been severely restricted because it decomposes in the temperature range 800–1280 °C[1,4,5,11–14] and it has very low fracture strength. Indeed tialite is stable from room temperature up to 750 °C[1,4] and from 1280 up to its melting temperature, being subject to a eutectoid decomposition to its parent oxides α-alumina and rutile between 750 and 1280 °C.[1] Its low fracture strength is due to the extensive microcracking occurring during cooling from the firing temperature.[1]

The material is isomorphous with pseudobrookite, crystallizing in the orthorhombic space group Cmcm[1,12] and is characterized by a pronounced anisotropy in thermal expansion coefficient resulting in a distinct hysteresis.[1,6,14] This pronounced anisotropy is the reason for the severe microcracking during cooling which leads to the poor mechanical properties of the sintered material.[14–17] The microcracking phenomenon is closely related to the material microstrucure.[9,15–17] Below a critical grain size, the elastic energy of the system is insufficient for microcrack formation

* Fax: +30-28210-37870.
E-mail address: athtse@mred.tuc.gr (A. Tsetsekou).

0955-2219/$ – see front matter © 2004 Elsevier Ltd. All rights reserved.
doi:10.1016/j.jeurceramsoc.2004.03.024

during cooling and thus the mechanical properties are considerably enhanced.[1] This critical grain size depends on the thermal history of the sample[15,16,18] and is in the range of 1–2 μm.[14,15,17–22] The density of microcracks increases drastically with grain size increase once above the critical size.[1,14–20] The microcracking phenomenon determines finally the thermal expansion behavior of the material as well as the thermal diffusivity, the strength and the elastic modulus.[1,2,7,8,11,14–23]

The decomposition phenomenon has been addressed through various oxide additives that form solid solutions with the aluminum titanate. The oxides that are considered to have a good stability effect are Fe_2O_3, MgO, SiO_2, ZrO_2, $ZrSiO_4$, La_2O_3.[2,4,7,10,11,13,14,24–30] Among them, Fe_2O_3 and MgO have been considered to be the most effective ones.[4,7,13,14,24–30] However, a quite high percentage of MgO (of the order of 10–25 mol%) is required for an effective stabilization, and even this could not keep the material stable for more than a hundred of hours at the temperature of the maximum decomposition rate (1100 °C).[7,14,27] Slightly better stability efficiency is reported with Fe_2O_3 additions,[4,13,24] which in some cases led to material stable for about 300 h of annealing at 1000 °C in an oxidizing atmosphere.[24] In all cases, the decomposition proceeds fast after an initial time period following a nucleation and grain growth mechanism and its rate varies with both the type of additive and the material particle size.[2,7,23] Recently, it has been recognized that the combined effect of MgO and SiO_2 enhance significantly the material stability.[6,31] In a recent work, very positive results in terms of stability were also obtained by the addition of feldspar.[11] The additives, besides the stabilization effect, have a considerable influence on the microstructure thus affecting the mechanical and thermal properties of the material.

Besides the decomposition problem, another important concern is the low strength of the material due to the microcracking phenomenon. A solution that is proposed is the development of composite structures including as a second phase mainly mullite,[3,5,6,8,12,15,31,32] whereas zirconia and alumina have been also reported.[18,33–41] Mullite incorporation in the structure strengthens significantly the material, reducing also the grain growth rate and thus decreasing the microcrack density in the material; it also exhibits a stabilization effect in the structure.[6,12,31] Various efforts have also been made to control the tialite structure and enhance the mechanical and thermal properties of the material by producing nanosized powders consisted of either a single phase doped tialite or a composite structure through chemical methods.[2,3,5,6,31,41–45]

The present work concerns an analytical and comparative study of the properties of porous ceramic tialite supports for applications mainly in the area of filters for soot traps or for hot gas clean-up. The work comprises the manufacturing of both doped tialite ceramics stabilized with various oxide additives and mullite–tialite composites. In the first case, the study concerned the effect of various additives based on magnesia and silica on the material properties (thermal expansion, mechanical strength, porosity) and thermal stability. The additives were pure magnesia, commercial talc (for achieving the combined effect of magnesia and silica) and a combination of talc and feldspar. Mullite composites varying in the mullite percentage were also manufactured using kaolinite as the mullite source; these were compared with the doped tialite ceramics.

2. Experimental

For tialite formation, calcined alumina (Nabaltec 115-25) of purity 99.5% and a mean particle size d_{50} of 4.6 μm and rutile powder (Aldrich Chemical Co. Inc., purity 99.9%) of a mean particle size of 1 μm were mixed in the proper stoichiometry. As stabilizing agents, various oxide raw materials were also added in the alumina–titania mixture. These included MgO (Aldrich Chemical Co. Inc., purity 99.9%) of either 8 or 3 wt.%, talc (Luzenac, Cyprus International Minerals Corp.) of 6 or 9 wt.%, or a mixture of talc and feldspar (Minerals of Northern Greece) of 3 wt.% each. Additionally, tialite–mullite composites were also produced by adding in the alumina–titania mixture, the appropriate quantity of kaolin hydrite. In this way, four different composite structures were investigated differing in the relative percentage of kaolin (Glomax LL, Amberger Kaolinwerke GmbH) and alumina added. The powders' molar ratio was adjusted in order to obtain after sintering tialite–mullite ceramics with 10, 15, 20, and 50 wt.% mullite. The raw materials were characterized by atomic absorption spectrophotometry (Varian Spectra AA.10) for the chemical composition evaluation, X-ray diffraction analysis (Siemens D500 Cu Kα radiation) and particle size distribution measurements (Malvern 3600E particle size analyzer). Table 1 summarizes the chemical composition and the mean particle size of the raw materials.

Table 1
Chemical compositions and particle size distributions of mineral raw materials

	SiO_2 (wt.%)	Al_2O_3 (wt.%)	MgO (wt.%)	Na_2O (wt.%)	K_2O (wt.%)	CaO (wt.%)	Fe_2O_3 (wt.%)	TiO_2 (wt.%)	Loss on ignition (1000 °C) (wt.%)	Particle size distribution		
										d_{10} (μm)	d_{50} (μm)	d_{90} (μm)
Talc	60.48	0.59	29.15	0.16	0.18	1.79	0.76	0.04	6.39	0.7	8	22
Kaolin	47.33	36.66	0.06	0.15	1.96	2.28	0.74	0.04	10.71	0.6	6.5	15
Feldspar	68.0	18.66	–	2.86	9.43	0.67	0.19	–	0.002	1	10	24
Alumina		99.5		0.2					0.15	2	4.6	9

For comparison purposes, cordierite ceramics using the same alumina, talc and kaolin powders as those employed for the tialite ceramics preparation (Table 1) in the proper stoichiometry were manufactured following exactly the same processing procedure as those for the tialite ceramics.

Initially, for achieving a homogeneous mixing of the constituents, the powder mixtures were wet ball milled for 2 h in ethanol with alumina balls in a Teflon jar. This procedure, after drying of the powder mixture, was followed by the subsequent addition of 4 wt.% (on powder basis) binder (methyl-hydroxy-propyl-cellulose MHPC 2000) and 2 wt.% (on powder basis) Na-stearate as dispersant and lubricant as well as the appropriate amount of deionized water and careful shear mixing under vacuum in a z-blade mixer. The resulting ceramic pastes were extruded to form rod-shaped samples by using a laboratory piston extruder fitted in an INSTRON 8562 mechanical testing machine. The rods after careful drying were fired in the temperature range 1350–1600 °C for 2 h with a heating rate of 2 °C/min and furnace cooled. Then they were characterized in terms of their physicochemical properties. The cordierite rods were fired at 1360 °C for 2 h using the same heating and cooling rates. The porosity in this case was adjusted by slightly varying the percentage of the water added in the initial powder mixture.

The phase composition after sintering was carried out by X-ray diffraction analysis employing a Siemens D500 Diffractometer (Cu Kα radiation). The samples' microstructure and morphology were evaluated by Scanning Electron Microscopy (SEM) using a Jeol JSM 6300 instrument combined with Energy Dispersive X-ray Microanalysis (EDS) (Link ISIS 300B Detector). Secondary (SEI) and backscattered electron images (BEI, COMPO mode) as well as X-ray mapping images were taken. The behavior during sintering was evaluated on the green samples by employing a Netzsch DIL 402C dilatometer. Thermal expansion coefficient studies were also performed on the sintered samples using the same instrument. In both cases, a constant heating rate of 5 °C/min was employed and a sapphire standard was used. For the mechanical properties evaluation, four-point bending tests were carried out in an Instron 8562 testing machine. The values were estimated by averaging six measurements for each sample type (rods of 1 cm diameter and 10 cm length), while bending was conducted at a crosshead speed of 1 mm min^{-1}. Porosity and pore size distribution were measured in a Quantachrome (Autoscan 33) Mercury porosimeter. Aging studies for investigating the stability of the tialite phase in the various compositions synthesized were also carried out. For this purpose, the samples were kept at 1000 °C for up to 1000 h in an air atmosphere. Samples, after aging at intermediate time periods, were taken out of the furnace and were characterized by X-ray diffraction analysis. A full characterization of the annealed samples (SEM studies, thermal expansion coefficient measurement, mineralogical analysis by XRD, porosity measurement, four-points bending test) was also carried out, which is presented in part II of this work. The compositions investigated for aging were the composite structures with 10, 15 and 20 wt.% mullite as well as the tialite ceramics stabilized with 8 wt.% MgO, 3 wt.% MgO and 6 wt.% talc.

3. Results and discussion

3.1. Dynamic sintering

Dilatometric analyses on the raw samples after their shaping and drying are shown in Fig. 1, whereas the various transformation phenomena occurring are described in Tables 2 and 3. Comparing the shrinkage curves of the MgO containing samples (Fig. 1a) with those of the talc or the talc–feldspar containing samples (Fig. 1b, Table 2) it is easily noticed that the addition of talc to the alumina–titania mixture leads to a higher shrinkage rate at the initial stages, whereas the maximum shrinkage rate in all cases is observed at around 1450 °C.

Different behavior during sintering is shown by the samples in which the kaolin was added for the formation of mullite (Fig. 1c), with the densification being more pronounced as the kaolin percentage in the structure increases. The phase transformation phenomena observed (Table 3) end to a continuous volume expansion occurring around the eutectic of Al_2O_3–SiO_2–TiO_2 (1470 °C),[13] which increases as mullite percentage in the structure increases. This observation leads to the conclusion that the phenomenon at the final stages of firing proceeds through a liquid phase sintering process,

Table 2
Phenomena observed in the doped tialite samples during dynamic sintering

Description	3 wt.% MgO	8 wt.% MgO	6 wt.% talc	3 wt.% talc + 3 wt.% feldspar	Attribution
Shrinkage start (°C)	850	910	800	800	
First expansion peak in the shrinkage rate curve (°C)	1056	1042	1128	1128	Formation of magnesium titanate phases[7]
Second expansion peak in the shrinkage rate curve (°C)	1254	1278	1300	1293	Tialite formation
Third expansion peak in the shrinkage rate curve (°C)	1355				Eutectic point of MgO–Al_2O_3–TiO_2[13]
Observation of maximum shrinkage (°C)	1490	1430	1455	1455	

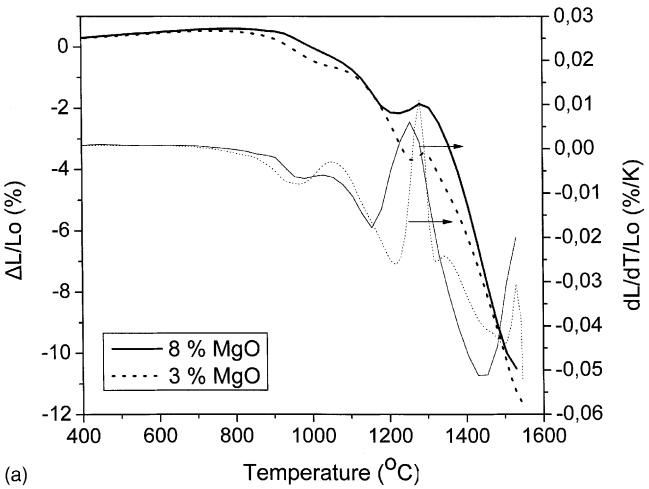

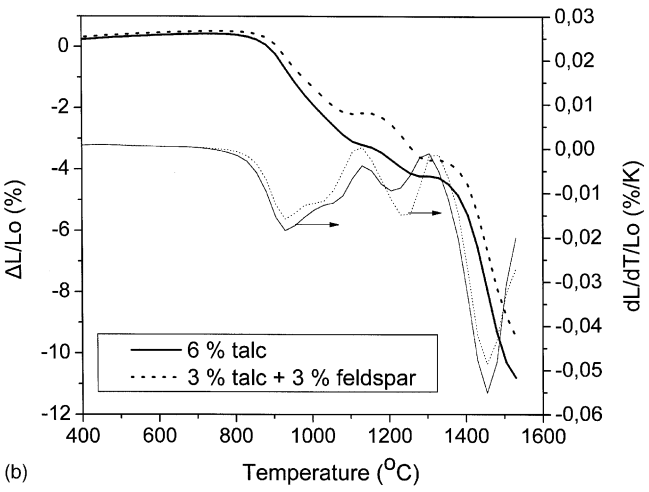

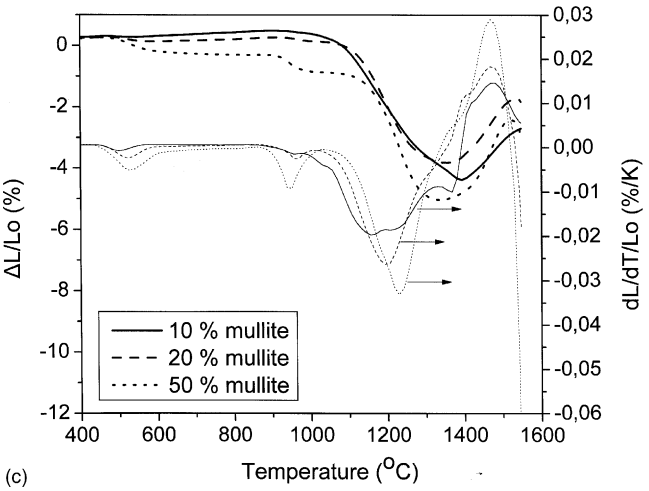

Fig. 1. Dilatometric studies on unfired tialite and tialite–mullite samples: (a) MgO doped samples, (b) talc and talc plus feldspar doped samples and (c) samples in which kaolin has been added for tialite–mullite composites preparation. Coarse lines: shrinkage curves, fine lines: first derivatives of the shrinkage curves.

because of which a fast shrinkage as observed in the dilatometric curves starts rapidly especially for the high mullite content samples.

Comparison of the temperature for tialite formation in the tialite–mullite composites, which was around 1350–1400 °C (Table 3) with those observed in the case of samples which did not contain mullite which were at about 100 °C lower (Table 2), suggests that the mullite presence in the ceramic structure delays significantly the tialite formation. This transformation is not complete up to about 1500–1550 °C, since the expansion is continued up to that point.

3.2. X-ray diffraction analysis

The phases detected in all the ceramics examined by X-ray diffraction analysis are summarized in Table 4; the XRD patterns obtained for some samples (8 wt.% MgO doped samples, 10 and 50 wt.% tialite–mullite composites) after firing at three different temperatures (1350, 1400 and 1600 °C) are depicted in Fig. 2. The XRD results are in good agreement with the dilatometric results concerning the formation temperature of the tialite phase.

Indeed, in all the cases of doped tialite compositions, tialite has been already formed after firing at 1350 °C, although the transformation reaction is not yet totally complete (Fig. 2a, Table 4). The reaction proceeds to almost its completion after firing at 1400 °C, whereas very pure samples (in which only tialite or tialite along with some traces of corundum could be detected) are found after sintering at higher temperatures (up to 1600 °C), this being true for all the tialite ceramics examined irrespectively of the stabilizing oxide (Table 4).

In the case of the composite structures of tialite–mullite, the mullite has been already formed after firing at the relatively low temperature of 1350 °C. However, in the low mullite content (10 wt.%) composite (Fig. 2b) the splitting of the (1 2 0) and (2 1 0) peaks of the orthorhombic phase is not complete a fact that only occurs after firing at 1600 °C. In the higher mullite content composites, this splitting of peaks is clearly observed even in the sample fired at 1350 °C (Table 4) with their height, however, increasing furthermore with firing temperature. This phenomenon indicates that the mullite transformation is not yet complete at 1350 °C but it is completed at lower temperature as the mullite content increases in the composites. Similarly the tialite formation becomes slower with increase in the mullite content. For the low mullite content samples, tialite peaks can be detected even in the samples fired at 1350 °C, which is not the case in the 50 wt.% mullite composite (Fig. 2c) for which no tialite peaks could be detected in the samples sintered at temperatures lower than 1400 °C. At these relatively low temperatures, unreacted alumina and rutile peaks of considerable height can be also detected along with tialite, which however are significantly reduced in height as the firing temperature increases resulting in either traces (low mullite content samples) or small peaks (50 wt.% mullite composite) after

Table 3
Phenomena observed in the tialite–mullite samples during dynamic sintering

Description	10 wt.% mullite	20 wt.% mullite	50 wt.% mullite	Attribution
Volume change (°C)	500–600	500–600	500–600	Dehydration of kaolin
Shrinkage start (°C)	900	900	900	
Plateau in the shrinkage curve (°C)	1000–1080	1000–1080	1000–1080	Spinel formation and crystallization of primary pseudotetragonal mullite[5,28]
First expansion peak in the shrinkage rate curve (°C)	1158	1201	1229	Crystallization of orthorhombic mullite[28]
Second expansion peak in the shrinkage rate curve (°C)	1410	1410	The peak is overlapped by the third one	Tialite formation
Third expansion peak in the shrinkage rate curve (°C)	1470	1470	1470	Eutectic point of Al_2O_3–SiO_2–TiO_2[13]
Start of fast shrinkage (°C)	>1550	1540	1520	

firing at 1600 °C (Table 4). From this result, it is clear that the kaolin addition shifts the tialite formation to higher temperatures and this shift is more pronounced as the kaolin content in the initial composition increases, a fact that was also discussed when analyzing the dilatometric curves.

3.3. Study of the physical and mechanical properties

The results of porosity measurements as well as of four-point bending tests in the samples fired at different temperatures are described in Tables 5 and 6 for the tialite ceramics and for the tialite–mullite composites respectively; porosity data are plotted in Fig. 3. Table 7 presents the porosity and bending strength of cordierite ceramics, which were prepared for comparison purposes.

Porosity measurements (Fig. 3a) lead to similar conclusions as those derived from the dilatometric results. The MgO doped samples show a slow but constant decrease of porosity with temperature, with the higher MgO content sample densifying more rapidly. An even higher densification rate at the initial firing stages is observed in the samples with the talc additions, although that the final porosity value, in this case, remains high after firing at 1600 °C. The densification of tialite–mullite composites delays considerably. An abrupt decrease in porosity in the samples with 20 and 50 wt.% mullite, however, is observed at 1600 °C, which is more pronounced in the high kaolin content sample, indicating the increased presence of liquid phase during sintering in these samples in agreement with the dilatometric results.

It should be pointed out that the composite structures with 10–20 wt.% mullite fired in the temperature range 1500–1600 °C exhibit the appropriate open porosity values (30–35%) for honeycomb monoliths fabrication for filters or catalyst supports construction, while at the same time, they show a satisfactory mechanical strength (20–40 MPa) for such applications. Mercury porosimetry measurements on the samples fired at 1600 °C showed that the mean pore size is ranged between 1 and 2 μm depending on their composition (Fig. 3b).

Studying Tables 5 and 6, a decrease of strength with sintering temperature is observed due to the progressive formation of the weak tialite phase.[11,15,21,35] This is especially true for the doped tialite ceramics that show an initial very rapid reduction of strength despite the porosity reduction, the results depending however on both the stabilizing agent and its addition percentage. Among all the compositions of doped tialite ceramics, those doped with 3 wt.% MgO show the worst behavior, whereas the talc stabilized samples show quite satisfactory values especially in the low sintering temperatures. Even better mechanical properties are measured in the tialite–mullite composites. It is worth noting in this case observing the porosity values of Table 6 in relation

Table 4
Phases detected by XRD in the doped tialite and tialite–mullite ceramics sintered at different temperatures

Additive in sample	Sintering temperature (°C)		
	1350	1400	1600
3 wt.% MgO	T, A(vs), R(tr)	T, A(tr)	T, A(tr)
8 wt.% MgO	T, A(vs), R(tr)	T, A(tr)	T
6 wt.% talc	T, A(vs)	T, A(tr)	T
9 wt.% talc	T, A(vs)	T, A(vs)	T, A(tr)
3 wt.% talc + 3 wt.% feldspar	T, A(vs), R(vs)	T, A(vs), R(tr)	T, A(tr)
10 wt.% mullite	M, T, A, R	M, T, A(s), R(s)	OM, T, A(tr)
20 wt.% mullite	OM, T, A, R	OM, T, A(s), R(s)	OM, T, A(tr)
50 wt.% mullite	OM, A, R	OM, T(s), A, R	OM, T, A(s), R(s)

T: tialite, A: α-alumina, R: rutile, M: mullite (not complete splitting of the (1 2 0) and (2 1 0) peaks of the orthorhombic mullite), OM: orthorhombic mullite. (s): small peak, (vs): very small peak, (tr): traces.

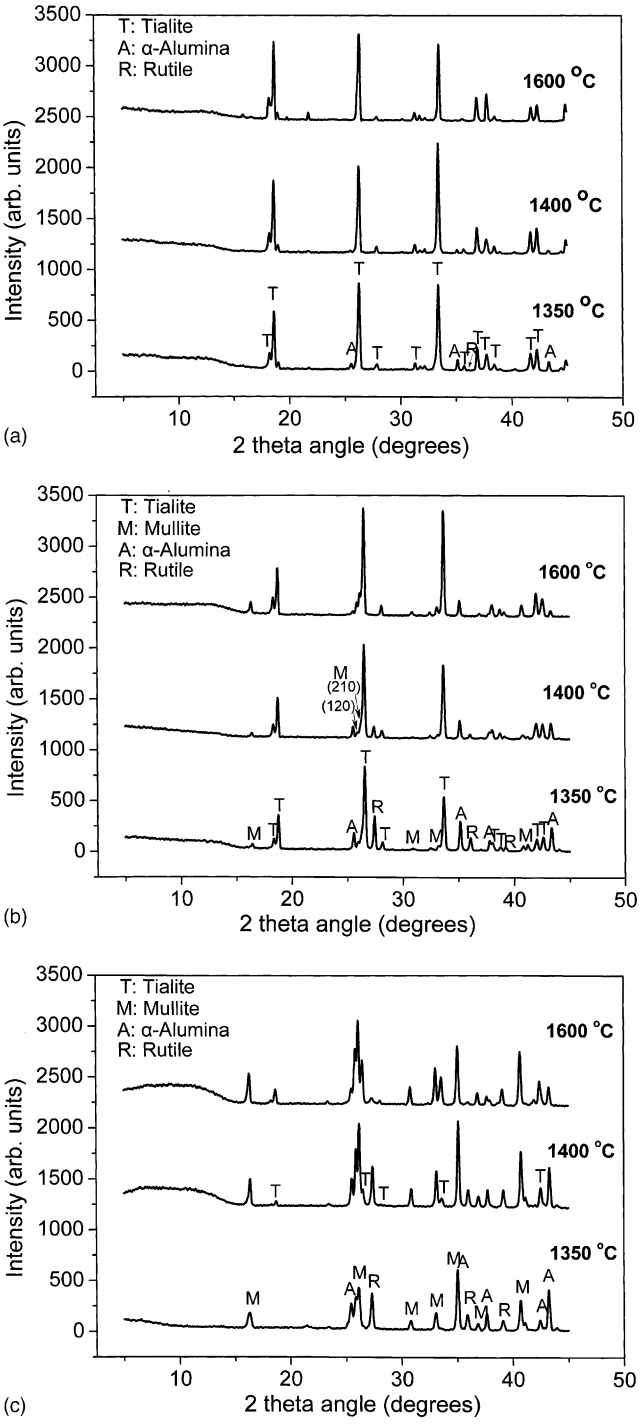

Fig. 2. X-ray diffraction patterns of tialite ceramics and tialite–mullite composites after firing at 1350, 1400 and 1600 °C: (a) tialite ceramics stabilized with 8 wt.% MgO, (b) 10 wt.% mullite composites and (c) 50 wt.% mullite composites.

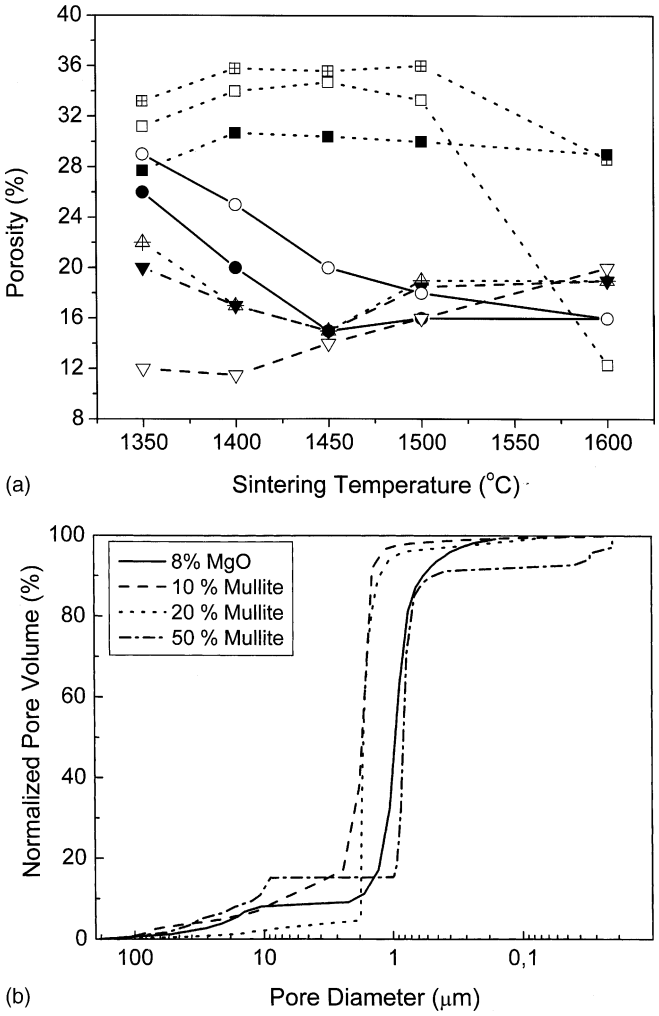

Fig. 3. Tialite ceramics and tialite–mullite composites pore structure characteristics: (a) open porosity vs. firing temperature and (b) pore size distribution of tialite ceramics and tialite–mullite composites fired at 1600 °C. (●) 8 wt.% MgO doped sample, (○) 3 wt.% MgO doped sample, (▼) 6 wt.% talc doped sample, (⏃) 3 wt.% talc plus 3 wt.% feldspar doped sample, (▽) 6 wt.% talc doped sample, (■) 10 wt.% mullite composite, (⊞) 20 wt.% mullite composite, (□) 50 wt.% mullite composite.

to the bending strength, that in all the composite materials examined, generally the strength increases with the reduction of porosity, thus the problem of strength reduction despite the densification observed in the doped tialite ceramics being overcome in the composite materials. Indeed, although a small strength reduction can be also seen in the composites in the initial firing stages, the porosity in this case remains almost constant up to the firing temperature of 1500 °C (Fig. 3a).

Comparing the variation of bending strength of cordierite ceramics versus porosity as presented in Table 7, to that of tialite ceramics or tialite–mullite composites already discussed, it can be concluded that tialite–mullite composites with 10 or 20 wt.% mullite present better or comparable bending strength to that of cordierite (bending strength 23–30 MPa) at the same porosity range (27–30%).

Thermal shock resistance characterizations including very rapid firing with oxy-acetylene flame and abrupt quenching in water confirmed the high resistance of these structures. The 10 wt.% mullite composite was not broken after repeating three times this very severe thermal shock test, while the

Table 5
Effect of stabilizer and its percentage on the properties of tialite ceramics

Temperature (°C)	3 wt.% MgO			8 wt.% MgO			9 wt.% talc			6 wt.% talc			3 wt.% talc + 3 wt.% feldspar		
	P (%)	*σ* (MPa)	*E* (GPa)	*P* (%)	*σ* (MPa)	*E* (GPa)	*P* (%)	*σ* (MPa)	*E* (GPa)	*P* (%)	*σ* (MPa)	*E* (GPa)	*P* (%)	*σ* (MPa)	*E* (GPa)
1350	29	17.4 ± 1.3	9.7 ± 0.9	26	38.4 ± 2.5	15.5 ± 1.2	12	22.9 ± 1.4	27.4 ± 2.0	20	48.5 ± 3.0	21.4	22	34.7 ± 2.2	13.3 ± 1.0
1400	25	16.3 ± 1.0	5.5 ± 0.4	20	34.0 ± 2.1	9.6 ± 0.7	12	17.3 ± 1.1	14.3 ± 1.0	17	19.5 ± 1.1	15.4	17	13.8 ± 1.9	8.3 ± 1.3
1450	20	13.7 ± 0.8	4.0 ± 0.3	15	27.8 ± 1.6	6.0 ± 0.4	14	29.1 ± 1.7	12.0 ± 0.8	15	22.2 ± 1.2	7.7	15	28.1 ± 1.8	8.8 ± 0.7
1500	18	13.1 ± 0.9	7.6 ± 0.6	16	26.6 ± 1.5	7.6 ± 0.5	16	22.7 ± 1.4	10.5 ± 0.8	18	22.5 ± 1.4	7.9	19	18.6 ± 0.9	7.4 ± 0.4
1600	16	16.8 ± 1.2	3.5 ± 0.3	16	19.3 ± 1.1	2.5 ± 0.2	20	14.0 ± 1.0	5.1 ± 0.4	19	14.7 ± 1.0	5.5	19	15.9 ± 1.0	4.0 ± 0.3

P: porosity, *σ*: bending strength, *E*: modulus of elasticity.

20 wt.% mullite composite was broken during quenching in water after the second thermal shock treatment. However, the 50 wt.% mullite composite did not withstand this treatment and it was broken during the first heating step with the oxy-acetylene flame.

The conclusion derived is that the composite structures with 10–20 wt.% mullite fired in the temperature range between 1500 and 1600 °C exhibit the appropriate open porosity values (30–35%) for honeycomb monoliths fabrication, while at the same time, they show a satisfactory bending strength (20–40 MPa) for such applications.

3.4. Microstructure studies

The microstructure of the tialite samples fired at different temperatures as it was observed under SEM is shown in Fig. 4. Sintering at 1350 °C leads to a very fine structure in all cases. Among them the 6 wt.% talc stabilized sample exhibits the finer and more homogeneous structure consisting of grains with a mean size in the order of 1–3 μm (Fig. 4a and b). The appearance of the sample doped with talc plus feldspar is almost the same, however a wider grain size distribution is observed since in some rare cases the grain size has already reached 10 μm (Fig. 4c and d). The 8 wt.% MgO doped sample is also of very fine structure consisting of both plate like and elongated grains with a mean size at 3 μm (Fig. 4e). No microcracks could be observed in these samples except for the talc plus feldspar sample in which some isolated microcracks appear (Fig. 4d). Microcracking phenomenon in tialite ceramics is widely recognized to occur when the microstructure consists of grains larger than a critical grain size, which lies in the range 1–2 μm[14,15,17–22] and this is the case for the samples that are discussed now except for the talc plus feldspar one which had in some cases exceeded this threshold. Firing at 1450 °C, however, has promoted the grain growth. Grains of the order of 10 μm are found along with smaller ones leading to increased inhomogeneity and the first transgranular microcracks are detected (Fig. 4f for 8 wt.% MgO doped sample). When firing temperatures increase furthermore a remarkable grain growth occurs in all the cases accompanied with extensive microcracking (Fig. 4g and h for the 8 wt.% MgO and 6 wt.% talc doped sample, respectively). This appearance could easily explain the decrease in strength observed as the sintering temperature increases despite the densification process.

Scanning Electron Microscopy studies (Fig. 5) were also performed on the tialite–mullite composite structures in order to compare them with the doped tialite ceramics and better understand their mechanical behavior. All the composites present a very fine structure even after firing at 1600 °C (Fig. 5a) with the structure becoming finer as the mullite content in it increases (Fig. 5b–d). Some very rare and very small microcracks can hardly be seen in the low content mullite samples fired above 1450 °C. It is obvious that mul-

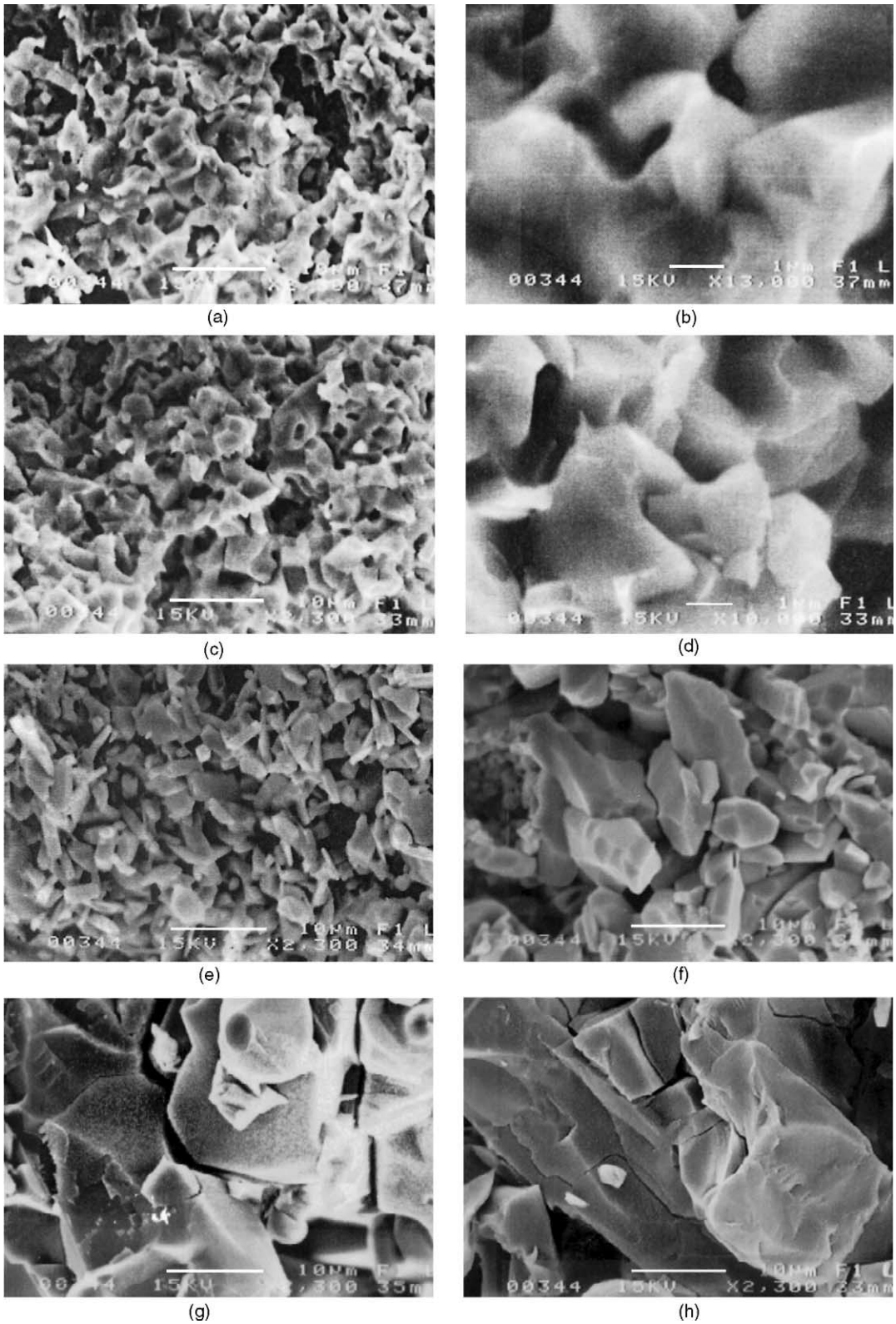

Fig. 4. Tialite ceramics microstructure (SEI images): (a) and (b) 6 wt.% talc doped sample fired at 1350 °C at a magnification: (a) 2300×, (b) 13,000×; (c) and (d) 3 wt.% talc + 3 wt.% feldspar doped sample fired at 1350 °C at a magnification: (c) 2300×, (d) 10,000×; (e), (f) and (g) 8 wt.% MgO doped sample at a magnification 2300× fired at: (e) 1350 °C, (f) 1450 °C, (g) 1600 °C; and (h) 6 wt.% talc doped sample fired at 1600 °C (magnification 2300×).

Table 6
Porosity and mechanical properties of tialite–mullite composites

Temperature (°C)	10 wt.% mullite			20 wt.% mullite			50 wt.% mullite		
	P (%)	σ (MPa)	E (GPa)	P (%)	σ (MPa)	E (GPa)	P (%)	σ (MPa)	E (GPa)
1350	28	37.5 ± 2.4	19.9 ± 1.5	33	59.9 ± 3.0	37.3 ± 2.3	31	79.8 ± 2.9	36.3 ± 1.6
1400	31	28.0 ± 1.8	39.1 ± 3.0	36	42.0 ± 1.9	22.4 ± 1.3	34	81.0 ± 3.4	16.1 ± 0.8
1450	30	23.0 ± 1.4	12.4 ± 0.9	36	38.1 ± 1.9	21.9 ± 1.4	35	62.6 ± 2.7	40.4 ± 2.1
1500	30	22.7 ± 1.2	13.3 ± 0.8	36	35.3 ± 2.0	19.7 ± 1.3	33	64.0 ± 2.5	42.6 ± 2.0
1600	29	21.0 ± 0.9	8.9 ± 0.5	29	36.5 ± 1.7	19.9 ± 1.1	12	120.0 ± 3.5	54.7 ± 2.0

P: porosity, σ: bending strength, E: modulus of elasticity.

Table 7
Porosity and bending strength of cordierite ceramics

Porosity (%)	Bending strength (MPa)
27	30.5 ± 2.3
28	27.5 ± 1.1
29	25.5 ± 1.4
30	23.2 ± 1.3

Firing temperature: 1360 °C.

lite additions hinder considerably the grain growth process, a result that is also reported in the literature,[3,6,8,12,28] affecting positively by this way the mechanical properties. Another important observation is the homogeneous distribution of very fine equiaxed mullite grains, of the order of 2–3 μm in size, which are embedded into the structure of tialite as it is shown in Fig. 6a and b.

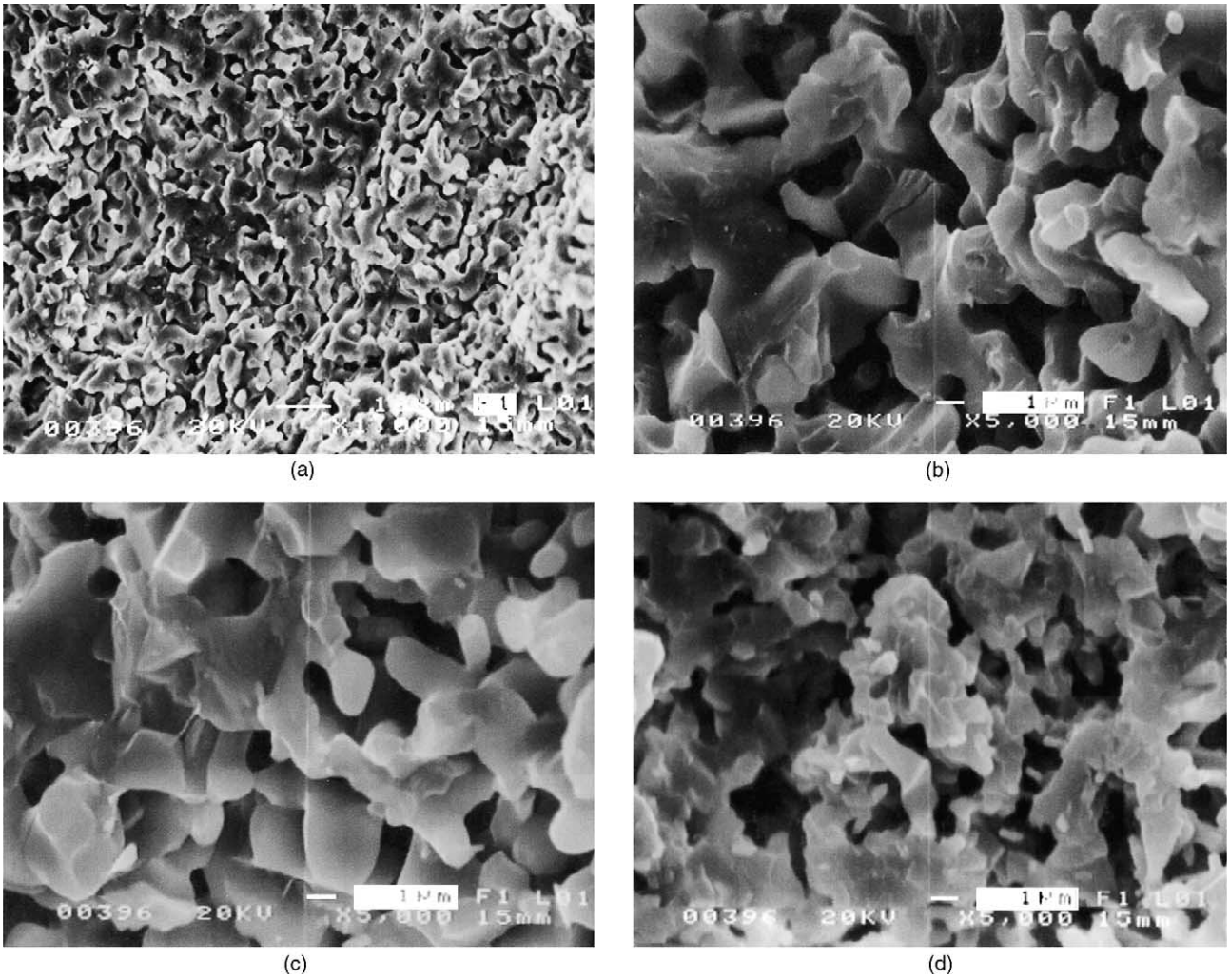

Fig. 5. Tialite–mullite composites microstructure: (a) SEI image (2000×) of a 10 wt.% mullite composite fired at 1600 °C; (b), (c) and (d) SEI images at a higher magnification (5000×) of various tialite–mullite composites fired at 1500 °C: (b) 10 wt.% mullite composite, (c) 20 wt.% mullite composite and (d) 50 wt.% mullite composite.

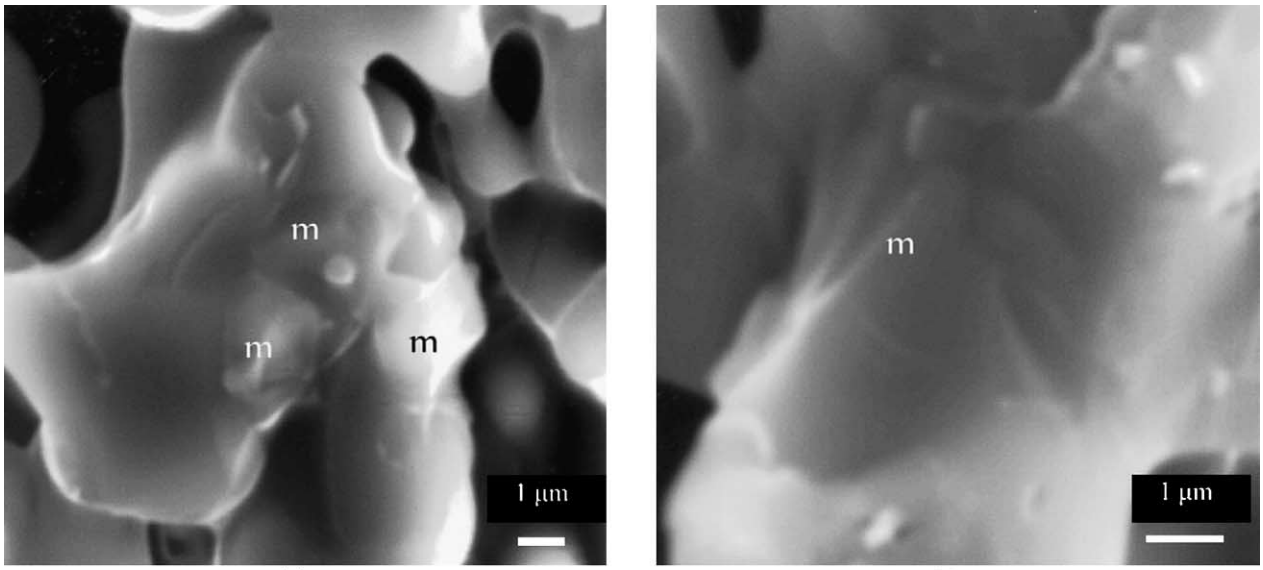

Fig. 6. Details of tialite grains in tialite–mullite composites fired at 1600 °C: (a) 15 wt.% mullite composite (SEI 9000×) and (b) 10 wt.% mullite composite (SEI 15,000×): mullite grains (marked with m) can be observed attached to them.

3.5. Thermal expansion behavior

Measuring of the thermal expansion behavior of the ceramics developed is in agreement with the already discussed results. In Fig. 7a the thermal expansion coefficient as a function of temperature is plotted for all the different compositions examined after sintering at 1600 °C. The reference temperature for obtaining the thermal expansion coefficient values is 30 °C. The MgO doped samples show the highest values among the doped tialite ceramics, approaching those of the undoped tialite as the MgO percentage increases, in agreement with theoretical calculations suggesting almost similar axial thermal expansion coefficients of the $Al_{1.62}Mg_{0.19}Ti_{1.19}O_5$ solid solution as those of Al_2TiO_5 in all three axes.[4] On the contrary, it is easily observed in this diagram that the talc containing samples present in all cases almost the same behavior while showing the lowest thermal expansion values.

Almost similar thermal expansion values as those of the 8 wt.% MgO doped tialite samples are obtained when measuring the 10 wt.% mullite sample, despite the presence of the higher expansion phase of mullite. However, as expected, the mullite presence in the structure leads to a constant increase of the thermal expansion coefficient values as its percentage increases. Nevertheless, the values of the thermal expansion coefficient are still within acceptable limits for the applications under consideration. The 10 wt.% mullite composite has lower thermal expansion than cordierite while that of 15 wt.% mullite somewhat higher.

In order to better understand the thermal expansion behavior, the expansion curves of the various compositions are also plotted and compared. In Fig. 7b, a comparison of the thermal expansion behavior of the MgO doped samples, with that of the undoped tialite is tried. The undoped tialite sample shows the characteristic behavior of this material contracting at first during heating due mainly to the progressive closing of microcracks and then at above about 400 °C starting to expand, as the larger thermal expansion coefficients begin to dominate.[1] A small contraction at about 1100 °C suggests that some decomposition of the material may occur. During cooling, the characteristic hysteresis loop appears with the sharp expansion below 600 °C, which is associated with the expansion and propagation of cracks.[1,5,7,14,17,18,26] The 3 wt.% MgO doped sample presents a delay in the expansion during heating which starts being observed at about 900 °C, and also the characteristic hysteresis loop during cooling, with the expansion starting at somewhat lower temperature. Increased expansion, as expected, is observed in the 8 wt.% MgO doped sample. Quite different behavior is seen in the talc stabilized samples (Fig. 7c) compared to the MgO doped ones. An increased contraction is observed at first followed by a more abrupt expansion that takes place in much higher temperatures, between 1100 and 1200 °C. The hysteresis loop is quite large, whereas in the cooling curve, below 500 °C, an abrupt expansion is observed characteristic of the extended microcracking of this kind of samples below that temperature. Exactly similar behavior is found in the literature[5] in tialite–mullite composites that have been developed under excess of silica. These samples[5] had shown lower thermal expansion coefficients compared to the sample without excess silica, with the sample with 3% excess silica exhibiting the lowest value. The turning temperature points in the cooling curves attributed to the reopening of microcracks were similarly sharp.

When comparing the thermal expansion curves of the 8 wt.% MgO samples fired at different temperatures in

Fig. 7d what is observed is a continuous decrease of the thermal expansion as the firing temperature increases up to 1500 °C. This according to literature studies can be attributed to the continuous increase of the grain size as the firing temperature increases, a fact that has been widely discussed.[2,7,8,19,20] A small reduction of the thermal expansion hysteresis loop is also observed in accordance to the works of Giordano et al.[14] and Kuszyk and Bradt,[20] whereas the turning point to expansion in the cooling curves is continuously shifted towards higher temperatures (from less than 400 to about 600 °C), a fact that can be attributed to the increased microcracks density with firing temperature. Indeed, hysteresis depends greatly on both the microstructure[15] and the crack volume,[22] with the grain size playing an important role.[14,20] In both those works,[14,20] the researchers have observed an initial increase of hysteresis, as the grain size increases up to a certain value which was estimated at 15 μm, but when the grain size exceeds this value, the hysteresis starts decreasing. However, when exaggerating grain growth occurs as in the case of the sample

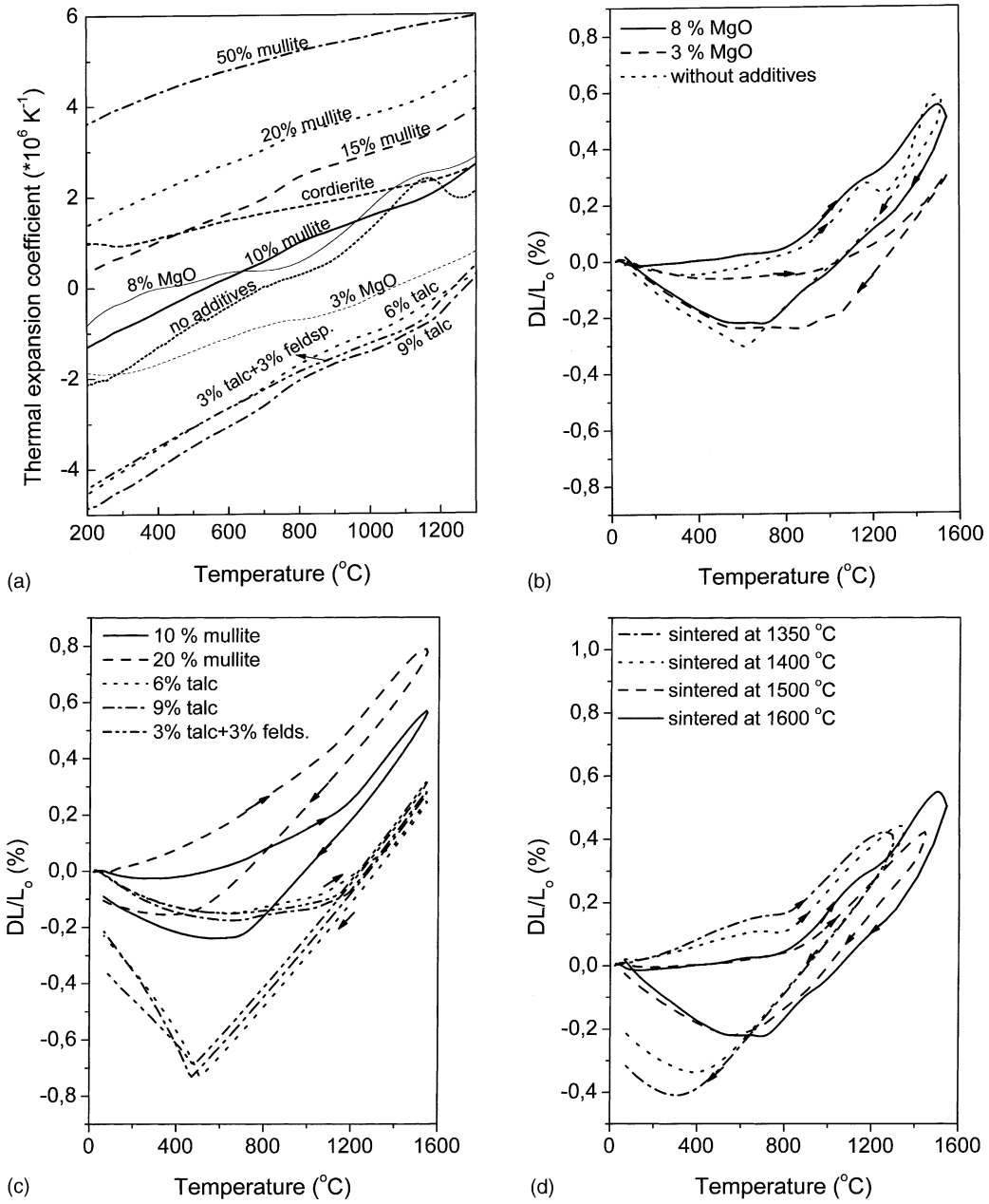

Fig. 7. Thermal expansion results of talcite and talcite–mullite ceramics: (a) thermal expansion coefficient curves of samples fired at 1600 °C, (b) thermal expansion behaviour of an undoped talcite sample and of MgO doped samples fired at 1600 °C, (c) thermal expansion behaviour of talc doped talcite samples and talcite–mullite composites fired at 1600 °C, (d) thermal expansion behaviour of MgO doped talcite samples fired at different temperatures, (e) thermal expansion behaviour of 10 wt.% mullite composites fired at different temperatures, (f) thermal expansion behaviour of 20 wt.% mullite composites fired at different temperatures.

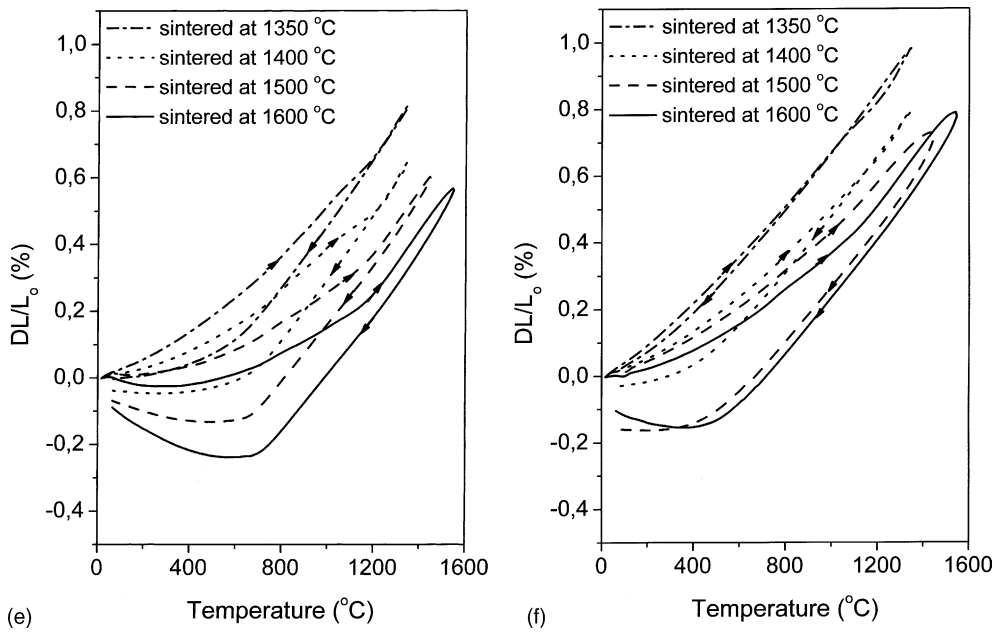

Fig. 7. (*Continued*).

sintered at 1600 °C (mean grain size at about 20 μm) the trend is exactly the opposite and the thermal expansion starts decreasing, according to Giordano et al.,[14] who claimed the increase of thermal expansion with the grain size enhancement for high mean grain sizes. The hysteresis loop in this case is enlarged and the turning point for expansion has been shifted upwards at about 750 °C.

A continuous decrease of the thermal expansion coefficient with firing temperature is also observed for the tialite–mullite composites in Fig. 7e and f. This decrease could be partly justified by the formation of tialite, which, in this case, occurs at higher temperatures as previously discussed and partly by the increase of the grain size with firing temperature. The hysteresis loop increases also with the increase in firing temperature, and as in the MgO doped samples the expansion turning point in the cooling curve as well as the sharpness of this change increase continuously, occurring at about 500 °C in the sample fired at 1350 °C and at about 750 °C in the sample fired at 1600 °C. The same behavior is noticed in the case of tialite–20 wt.% mullite composites (Fig. 7f). However the hysteresis loops are much narrower in this case, whereas it is worth noting the virtual absence of expansion in the cooling curve at the low temperature regime for the samples fired up to 1500 °C. What is only observed in this part of the curve is a change in the contraction rate which occurs at 400 °C (except for the sample fired at 1350 °C). The much less extent of microcracking in the composites is the reason for this behavior. This is reinforced by the fact that a small expansion starting at 500 °C in the cooling curve was observed only in the sample fired at 1600 °C, which exhibits the highest mean grain size among these samples.

3.6. Stability behavior—aging studies

The stability of the ceramics developed was evaluated by performing aging studies at 1000 °C. For comparison purposes the samples evaluated were those sintered at 1600 °C, as the aluminum titanate formation in them has been completed in all cases. The samples after their aging for different time intervals were characterized by X-ray diffraction analysis. Tialite decomposes progressively with the aging time leading to corundum and rutile formation. Thus, a reduction in the peak areas of tialite and an increase in corundum and rutile peak areas can be detected. The reduction in tialite intensity and the respective increase in rutile and corundum intensities are more pronounced in the case of MgO doped ceramics in which the formation of spinel can be also observed. In order to have an indication of the decomposition reaction rate, the ratio $(I_{\text{tialite}})/(I_{\text{tialite}} + I_{\text{rutile}})$ versus the aging time has been plotted in Fig. 8. In this ratio, the I_{tialite} and I_{rutile} refer to the integral intensities of the (0 2 3) β-tialite and (1 0 1) rutile peak, respectively. This ratio has been correlated in the literature[6,24,35] with the tialite decomposition percentage. The least stable sample is that with only 3 wt.% MgO addition, which shows a very fast decomposition since considerable amount of rutile can be detected even after 10 h of aging. On the contrary, the 8 wt.% MgO doped sample is almost stable up to 100 h of aging. However, this sample too, exhibits a fast decomposition after that time period leading to almost complete decomposition after about 500 h of aging. It seems that the MgO is extracted from the material structure reacting with the Al_2O_3 towards spinel, permitting, as a consequence, the tialite decomposition to corundum and rutile. A very encouraging behavior was shown by the 6 wt.% talc doped sample. This

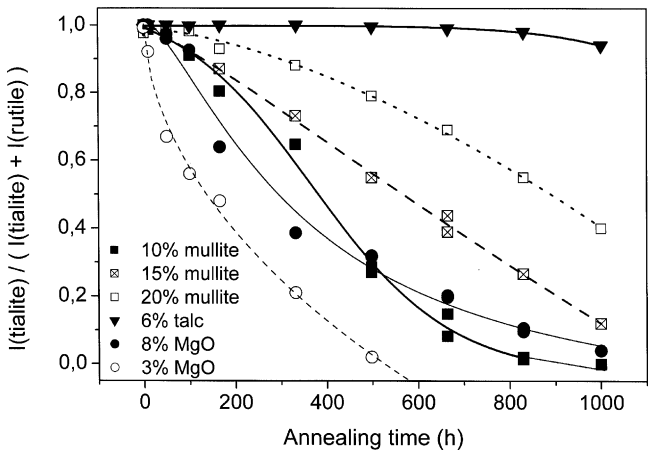

Fig. 8. X-ray relative integral intensity of tialite (2 3 0) peak vs. the sum of tialite (2 3 0) and rutile (1 0 1) peak integral intensities at various time periods after annealing at 1000 °C.

sample presents an excellent stability after about 800 h of aging. Then again the decomposition proceeds but with a rather slow rate so that only after 1000 h of aging a measurable amount of tialite has been decomposed. It seems that, in all cases, tialite decomposition starts after a certain nucleation period, which increases with the increase of the MgO addition percentage. However, the combined effect of MgO and SiO_2 of talc increase dramatically the nucleation time for tialite decomposition, leading to a significant increase of stability in this kind of sample, which remains stable for up to 800 h of aging. The study of the composites behavior showed similar results: tialite decomposition starts, in this case as well, after a certain nucleation period, which is more prolonged as the mullite content in the structure increases. Compared with the 8 wt.% MgO doped sample, the 10 wt.% mullite composite shows an increased nucleation time, however after that time the decomposition itself proceeds rather faster. As mullite content increases, the decomposition rate decreases; a fact, which combined with the prolonged nucleation period in these samples, suggests a progressively increased stability as mullite content increases. Indeed, the 20 wt.% mullite composite shows a rather good stability being stable up to 300 h of aging, followed by a fast decomposition afterwards. A first conclusion that can be derived is that talc is an excellent stabilizer, in contrast to MgO, which showed the less pronounced stability effect, while mullite has also a stabilizing effect delaying the tialite decomposition.

In part II of this work a detailed investigation of the decomposition rate at different temperatures is carried out and the properties of the materials after decomposition are discussed. Since talc proved an excellent stabilizer and mullite was also found having a considerable stabilizing effect, the addition of talc in tiallite–mullite composites for increasing stability is also discussed.

4. Conclusions

Tialite ceramics and tialite–mullite composites were prepared from commercial raw materials and were compared in terms of their properties for applications in the area of hot gas clean-up. Various oxide based materials such as MgO, talc, feldspar were investigated as stabilizing agents of tialite structure. The conclusions derived are summarized as follows:

- Both the type and the percentage of the stabilizing agent affect the final ceramic properties by influencing the ceramic microstructure. The MgO addition of 8 wt.% and the talc addition of 6 wt.% led to the production of ceramics with the best mechanical properties (22–26 MPa bending strength, at a porosity of about 16%, after firing at 1550 °C).
- In the case of MgO doped sample, the thermal expansion coefficient was comparable with that of cordierite, whereas the talc stabilized ceramics showed much lower values. Concerning thermal stability, talc proved the best stabilizer keeping the tialite structure stable up to 800 h of annealing at 1000 °C.
- Tialite–mullite composites of up to 20 wt.% mullite presented comparable thermal expansion coefficient to that of cordierite, which in combination with the considerably enhanced mechanical properties compared to both doped tialite ceramics and cordierite at the same porosity values, makes these composites excellent candidate materials for the applications under examination.
- The increased amount of mullite shifts the tialite formation at higher temperatures during firing. Additionally it was found that mullite presence has also a stabilizing effect delaying the tialite decomposition which is more pronounced as its percentage in the composite structure increases. For this purpose, in part II of this work, tialite–mullite composites stabilized furthermore by adding talc will be discussed.

References

1. Thomas, H. A. J. and Stevens, R., Aluminum titanate—a literature review. Part 1: microcracking phenomena. *Br. Ceram. Trans. J.* 1989, **88**, 144–151.
2. Nagano, M., Nagashima, S., Maeda, H. and Kato, A., Sintering behavior of Al_2TiO_5 base ceramics and their thermal properties. *Ceram. Int.* 1999, **25**, 681–687.
3. Popovskaya, N. F. and Bobkova, N. M., Mullite–tialite ceramic materials based on chemically precipitated mictures. *Glass Ceram.* 2002, **59**(7/8), 234–236 (a review).
4. Perera, D. S. and Cassidy, D. J., Thermal cycling of iron- and magnesium-containing aluminium titanate in a dilatometer. *J. Mater. Sci. Lett.* 1997, **16**, 699–701.
5. Huang, Y. X., Senos, A. M. R. and Baptista, J. L., Effect of excess SiO_2 on the reaction sintering of aluminium titanate −25 vol.% mullite composites. *Ceram. Int.* 1998, **24**, 223–228.

6. Huang, Y. X., Senos, A. M. R. and Baptista, J. L., Thermal and mechanical properties of aluminum titanate–mullite composites. *J. Mater. Res.* 2000, **15**(2), 357–363.
7. Buscaglia, V., Caracciolo, F., Leoni, M., Nanni, P., Viviani, M. and Lemaitre, J., Synthesis, sintering and expansion of $Al_{0.8}Mg_{0.6}Ti_{1.6}O_5$: a low-thermal-expansion material resistant to thermal decomposition. *J. Mater. Sci.* 1997, **32**, 6525–6531.
8. Yano, T., Kiyohara, M. and Otsuka, N., Thermal and mechanical properties of aluminum titanate–mullite composites (part 3)—effects of aluminum titanate particle size. *J. Ceram. Soc. Jpn. Int. Ed.* 1992, **100**, 487–492.
9. Jung, J., Feltz, A. and Freudenberg, B., Improved thermal stability of Al-titanate solid solutions. *Cfi DKG* 1993, **70**(6), 299–301.
10. Björkert, U.S., Mayappan, R., Holland, D. and Lewis, M. H., Phase development in La_2O_3 doped Al_2O_3: TiO_2 ceramic membranes. *J. Eur. Ceram. Soc.* 1999, **19**, 1847–1857.
11. Takahashi, M., Fukuda, M., Fukuda, M., Fukuda, H. and Yoko, T., Preparation, structure, and properties of thermally and mechanically improved aluminum titanate ceramics doped with alkali feldspar. *J. Am. Ceram. Soc.* 2002, **85**(12), 3025–3030.
12. Melendez-Martinez, J. J., Jimenez-Melendo, M., Dominguez-Rodriguez, A. and Wötting, G., High temperature mechanical behavior of aluminium titanate–mullite composites. *J. Eur. Ceram. Soc.* 2001, **21**, 63–70.
13. Liu, T. S. and Perera, D. S., Long-term thermal stability and mechanical properties of aluminium titanate at 1000–1200 °C. *J. Mater. Sci.* 1998, **33**, 995–1001.
14. Giordano, L., Viviani, M., Bottino, C., Buscaglia, M. T., Buscaglia, V. and Nanni, P., Microstructure and thermal expansion of Al_2TiO_5–$MgTi_2O_5$ solid solutions obtained by reaction sintering. *J. Eur. Ceram. Soc.* 2002, **22**, 1811–1822.
15. Hamano, K., Ohya, Y. and Nakagawa, Z., Crack propagation resistance of aluminium titanate ceramics. In *International Journal of High Technology Ceramics*. Elsevier Applied Science Publishers Ltd., Great Britain, 1985, pp. 129–137.
16. Ohya, Y., Nakagawa, Z. and Hamano, K., Crack healing and bending strength of aluminum titanate ceramics at high temperature. *J. Am. Ceram. Soc.* 1988, **71**(5), C232–C233.
17. Ohya, Y. and Nakagawa, Z., Grain-boundary microcracking due to thermal expansion anisotropy in aluminum titanate ceramics. *Am. Ceram. Soc. Commun.* 1987, **70**(8), C184–C186.
18. Hasselman, D. P. H., Donaldson, K. Y., Anderson, E. M. and Johnson, T. A., Effect of thermal history on the thermal diffusivity and thermal expansion of an alumina–aluminum titanate composite. *J. Am. Ceram. Soc.* 1993, **76**(9), 2180–2184.
19. Parker, F. J. and Rice, R. W., Correlation between grain size and thermal expansion for aluminum titanate materials. *J. Am. Ceram. Soc.* 1989, **72**(12), 2364–2366.
20. Kuszyk, J. A. and Bradt, R. C., Influence of grain size on effects of thermal expansion anisotropy in $MgTi_2O_5$. *J. Am. Ceram. Soc.* 1973, **56**(8), 420–423.
21. Cleveland, J. J. and Bradt, R. C., Grain size/microcracking relations for pseudobrookite oxides. *J. Am. Ceram. Soc.* 1978, **61**(11/12), 478–481.
22. Hennicke, H. W. and Lingenberg, W., Dependence of microstructure and physical properties of materials on the basis of aluminium titanate. W. Bunk: 2. *Inton. Symp. Ceram. Mater. Compon. Engines* 1986, **14–18**(4), 619–624.
23. Hwang, C. S., Nakagawa, Z. and Hamano, K., Microstructures and mechanical properties of TiO_2-doped alumina ceramics owing to decomposition of formed Al_2TiO_5. *J. Ceram. Soc. Jpn. Int. Ed.* 1994, **102**, 253–258.
24. Tilloca, G., Thermal stabilization of aluminium titanate and properties of aluminium titanate solid solutions. *J. Mater. Sci.* 1991, **26**, 2809–2814.
25. Djambazov, S., Lepkova, D. and Ivanov, I., A study of the stabilization of aluminium titanate. *J. Mater. Sci.* 1994, **29**, 2521–2525.
26. Thomas, H. A. J., Stevens, R. and Gilbart, E., Effect of zirconia additions on the reaction sintering of aluminium titanate. *J. Mater. Sci.* 1991, **26**, 3613–3616.
27. Buscaglia, V., Battilana, G., Leoni, M. and Nanni, P., Decomposition of Al_2TiO_5–$MgTi_2O_5$ solid solutions: a thermodynamic approach. *J. Mater. Sci.* 1996, **31**, 5009–5016.
28. Buscaglia, V. and Nanni, P., Decomposition of Al_2TiO_5 and $Al_{2(1-x)}Mg_xTi_{(1-x)}O_5$ ceramics. *J. Am. Ceram. Soc.* 1998, **81**, 2645–2653.
29. Buscaglia, V., Nanni, P., Battilana, G., Aliprandi, G. and Carry, C., Reaction sintering of aluminium titanate: I. Effect of MgO addition. *J. Eur. Ceram. Soc.* 1994, **13**, 411–417.
30. Buscaglia, V., Nanni, P., Battilana, G., Aliprandi, G. and Carry, C., Reaction sintering of aluminium titanate: II. Effect of different alumina powders. *J. Eur. Ceram. Soc.* 1994, **13**, 419–426.
31. Huang, Y. X., Senos, A. M. R. and Baptista, J. L., Preparation of an aluminium titanate −25 vol.% mullite composite by sintering of gel-coated powders. *J. Eur. Ceram. Soc.* 1997, **17**, 1239–1246.
32. Morishima, H., Kato, Z., Uematsu, K., Saito, K., Yano, T. and Ootsuka, N., Development of aluminum titanate–mullite composite having high thermal shock resistance. *J. Am. Ceram. Soc. Commun.* 1986, **69**(10), C226–C227.
33. Pratapa, S., Low, I. M. and O'Connor, B. H., Infiltration-processed, functionally graded aluminium titanate/zirconia–alumina composite. Part I: microstructural characterization and physical properties. *J. Mater. Sci.* 1998, **33**, 3037–3045.
34. Pratapa, S. and Low, I. M., Infiltration-processed, functionally graded aluminium titanate/zirconia–alumina composite. Part II: mechanical properties. *J. Mater. Sci.* 1998, **33**, 3047–3053.
35. Low, I. M. and Shi, C. G., Physical and thermal characteristics of aluminium titanate dispersed with β-spodumene and zirconia. *J. Mater. Sci.* 2000, **35**, 6293–6300.
36. Parker, F. J., Al_2TiO_5–$ZrTiO_4$–ZrO_2 composites: a new family of low-thermal-expansion ceramics. *J. Am. Ceram. Soc.* 1990, **73**(4), 929–932.
37. Lepkova, D., Pavlova, L. and Ivanova, J., Methods for composite material preparation in the zirconium–aluminium titanate system. *J. Mater. Sci. Lett.* 1997, **16**, 872–874.
38. Wohlfromm, H., Moya, J. S. and Pena, P., Effect of $ZrSiO_4$ and MgO additions on reaction sintering and properties of Al_2TiO_5-based materials. *J. Mater. Sci.* 1990, **25**, 3753–3764.
39. Kim, I. J. and Cao, G., Low thermal expansion behaviour and thermal durability of $ZrTiO_4$–Al_2TiO_5–Fe_2O_3 ceramics between 750 and 1400 °C. *J. Eur. Ceram. Soc.* 2002, **22**, 2627–2632.
40. Shimada, T., Mizuno, M., Katou, K., Nurishi, Y., Hashiba, M., Sakurada, O. *et al.*, Aluminum titanate–tetragonal zirconia composite with low thermal expansion and high strength simultaneously. *Solid State Ionics* 1997, **101–103**, 1127–1133.
41. Bartolome, J. F., Requena, J., Moya, J. S., Li, M. and Guiu, F., Cyclic fatigue crack growth resistance of Al_2O_3–Al_2TiO_5 composites. *Acta Mater.* 1996, **44**, 1361–1370.
42. Ibrahim, D. M., Mostafa, A. A. and Khalil, T., Preparation of tialite (aluminium titanate) via the urea formaldehyde polymeric route. *Ceram. Int.* 1999, **25**, 697–704.
43. Hareesh, U. S., Vasudevan, A. K., Mukundan, P., Damodaran, A. D. and Warrier, K. G. K., Low temperature sintering of seeded aluminium titanate precursor gels. *Mater. Lett.* 1997, **32**, 203–208.
44. Zaharescu, M., Crisan, M., Crisan, D., Dragan, N., Jitianu, A. and Preda, M., Al_2TiO_5 preparation starting with reactive powders obtained by sol–gel method. *J. Eur. Ceram. Soc.* 1998, **18**, 1257–1264.
45. Huang, Y. X. and Senos, A. M. R., Effect of the powder precursors characteristics in the reaction sintering of aluminum titanate. *Mater. Res. Bull.* 2002, **37**, 99–111.